0014-4754/96/090843-08$1.50 + 0.20

Research Articles

Freeze-induced shrinkage of individual cells and cell-to-cell propagation of intracellular ice in cell chains from salivary glands

W. K. Berger[a] and B. Uhrík[b,*]

[a] *I. Physiologisches Institut, Universität des Saarlandes, LKH, Bau 59, D-66424 Homburg (Germany)*
[b] *Institute of Molecular Physiology and Genetics, Slovak Academy of Sciences, Vlárska 5, 833 34 Bratislava (Slovakia), Fax +42 7 37 36 66, e-mail: bu@umfg.savba.sk*
Received 14 March 1996; received after revision 10 May 1996; accepted 19 June 1996

Abstract. The formation of intracellular ice (IIF), usually a lethal event to be avoided when cryopreserving cells, should, however, be enforced during the cryosurgical destruction of tumour cells. IIF has been investigated so far only in single cells in suspension. Because cells in tissues cannot be successfully cryopreserved, in contrast to single cells in suspension, the mechanism of IIF in tissues may depend on factors that facilitate IIF. We studied IIF in cell strands from salivary glands, which represent a simple form of a tissue. Their cells are connected by channels responsible for intercellular communication. A substantial fraction of cell dehydration during freezing occurs before cells are encapsulated by ice, and the degree of this pre-ice-front shrinkage appears to influence IIF. In strands with coupled cells IIF spread from one cell to adjacent cells in a sequential manner with short delays (200–300 ms), suggesting cell-to-cell propagation via intercellular channels. In strands pretreated with decoupling agents (dinitrophenol, heptanol), sequential IIF was absent. Instead, formation of ice was random, with longer and variable delays between consecutive darkenings indicating IIF. Results suggest that the mechanism of IIF spread, and consequently the degree of cryodamage in tissue, can be influenced by the presence of intercellular channels (gap junctions).
Key words. Salivary glands; cell strands; pre-ice-front shrinkage; intercellular communication; freeze-thaw cycle; intracellular ice.

IIF is usually a lethal event for living cells which are exposed to a freeze-thaw cycle. The probability of IIF is increased when water exosmosis of cells, which occurs during the formation of extracellular ice, is insufficient [1]. Cell dehydration during freezing has been investigated in suspensions of isolated cells by measuring the reduction of their cross-sectional areas under a cryomicroscope. Similar studies cannot be performed in cells within tissue because individual cells cannot be identified. It is likely that cells which are mechanically attached to each other and which are connected by intercellular channels (nexus or gap junctions), as in tissue, will shrink differently from isolated cells.

In simple cell arrangements such as cell chains or cell monolayers, freeze-induced reactions of interconnected individual cells can be studied even when cells are covered with ice. Though a cell chain represents a very simple tissue extending only in one direction, the influence of cell attachments and cell communication on events during freezing can be expected to be similar to those in three-dimensional tissue. We have studied the freeze-induced water exosmosis of individual cells and IIF in chains of cells dissected from isolated salivary glands of the larvae of *Chironomus thummi*. The possibility that gap junctions may influence the processes of cell shrinkage during freezing, of IIF and of intercellular spread of ice is worth studying in view of the role played by gap junctions in normal tissue functions, cell differentiation and tumour growth [2] and in view of the general interest in freezing processes in biology and medicine (cryofixation, cryoconservation, cryosurgery).

Materials and methods

Cell chains or gland segments consisting of 5–14 cells were dissected from isolated salivary glands of *C. thummi* larvae under a stereomicroscope either in the 'control medium' described by Politoff et al. [3] or in insect saline of the following composition (in mmol/l): KCl (2), disodium fumarate (28), $CaCl_2$ (5), NaCl (28), magnesium succinate (7), glutamine (80), TES (N-Tris[hydroxymethyl]methyl-2-aminoethane sulfonic acid) (5), NaOH (approx. 5) for adjustment to pH 7.4 (control medium), or NaCl (95), KCl (3), $CaCl_2$ (5), $MgCl_2$ (7), TES (5), pH adjusted with NaOH to 7.2 (insect saline). The excised strands usually adhered and became mechanically fixed to the underlying glass support by their own saliva (fig. 1). Prior to a freeze-thaw

* Corresponding author.

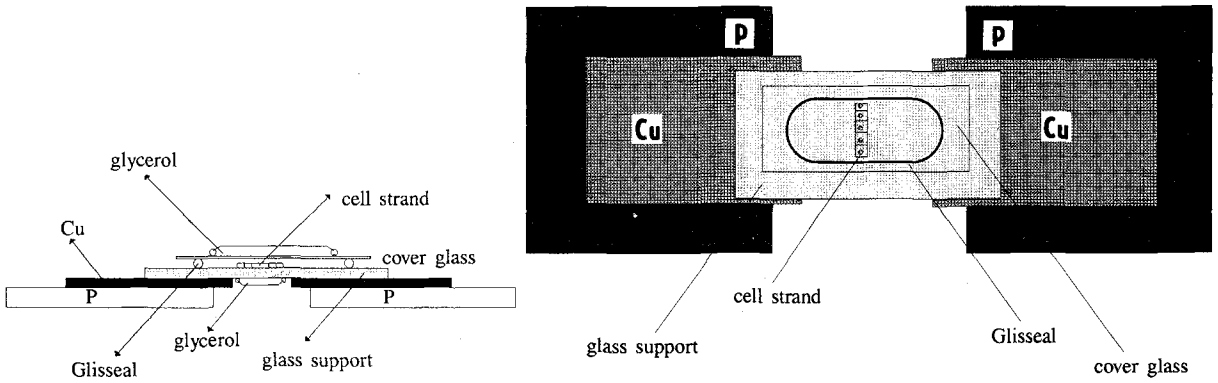

Figure 1. The sketch of the cryomicroscope freezing stage. Left: cross section. Right: top view. P = Peltier element, Cu = copper plate.

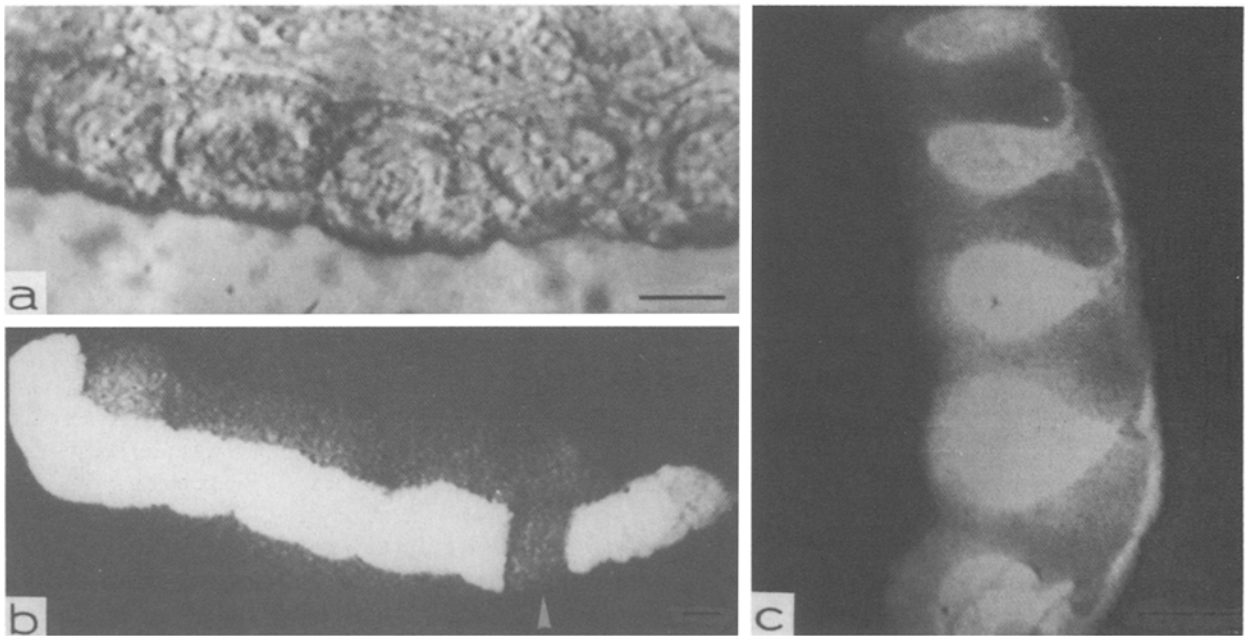

Figure 2. Micrographs of cell strands from salivary glands. (*a*) Bright-field image of a cell strand. (*b*) Another cell strand illuminated with epifluorescence optics. All but one cell displayed bright fluorescence. No fluorescein leaked from adjacent cells into the damaged nonfluorescent cell (arrowhead) during the observation time of 30 min. (*c*) The axis of this cell strand was now parallel to the advancing ice front (not shown). Cells had accumulated less fluorescein. The Ω-shaped contours of the central columns of the cells were visible. Clear outlines of the central cell portions as in figure 2c were only visible after the saliva between the cells – which also accumulated fluorescein – had been washed away. Bar: 40 μm.

cycle the strands were bathed in insect saline saturated with sodium fluorescein. After 15–20 min the fluorescein-containing saline together with the saliva between the cells was washed out with the fluorescein-free saline. After this treatment all undamaged cells were fluorescent when excited with blue light (fig. 2b and c).

The cell strand resting on the glass support was surrounded by a thin layer (10–12 mm in diameter) of laboratory grease (Glisseal). The top of this shallow experimental chamber was covered with a 15 × 20-mm glass cover (fig. 1). Fragments from a 30-μm glass fiber between the bottom and the roof of the chamber served as spacers to prevent accidental compression of the cells by the glass cover. The height of the chamber was selected by touching the glass cover with a needle until the highest part of the strand, consisting of flat cells, was touched. There was always a layer of fluid above the strand. For unimpeded observation of the cells during exposure to low temperatures, the upper and lower glass faces of the chamber were covered with a layer of glycerol. The condensing water mixed rapidly with the glycerol without significantly changing the optical properties of the protective layers during a freeze-thaw cycle. Both ends of the freezing chamber were placed on two Peltier elements for directional solidification [4]. Cooling one end of the glass slide established a thermal gradient which created an ice front in the saline moving from the cooled end towards the cell strand. At

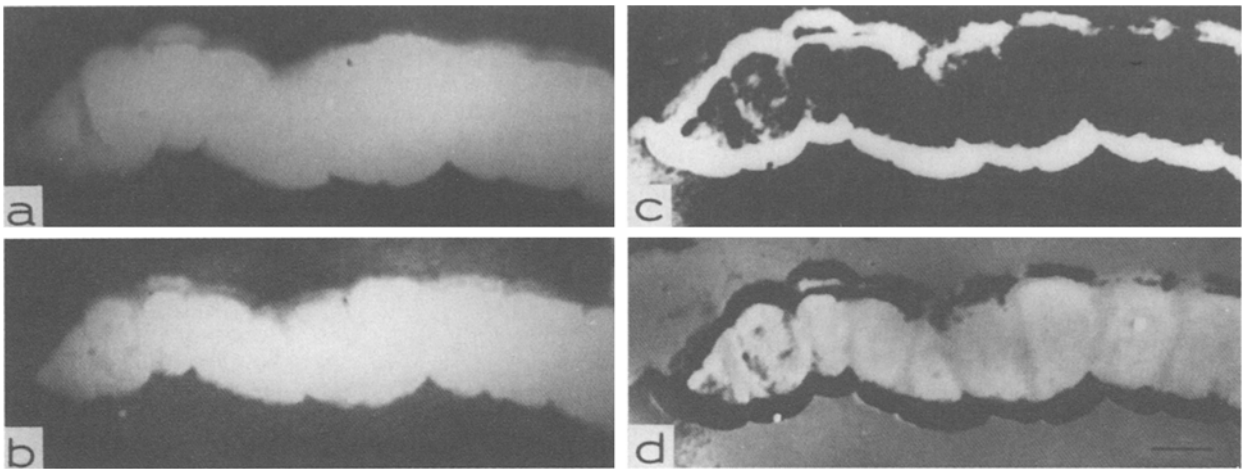

Figure 3. Images resulting from a stepwise application of the pixel-subtraction technique. (*a*) Digitized reference image of the cell strand before shrinkage. (*b*) Image of the same strand after freeze-induced shrinkage. The gray values of each pixel of (*b*) were then subtracted from the gray values of the corresponding pixels of (*a*) using an image-processing program (JAVA). The resulting subtraction image (*c*) representing the cell regions which had shrunken during freezing was stored on the computer. After displaying (*a*) again on the screen, the gray values of the pixels of (*c*) (the subtraction image) were subtracted from the gray values of the pixels in (*a*). This procedure was repeated three times. The shrunken regions appeared now as black bands in the periphery of the cells (*d*). Bar: 40 µm.

the beginning of the freezing process the cooling rate of approx. 1 °C/min was used. At subzero temperatures only the ice-front velocity (and not the cooling rate) was controlled by adjusting the temperature gradient. The currents to the Peltier elements were changed manually to keep the ice-front velocity approximately constant. Two ice-front velocities were used: a 'low' velocity for observing pre-ice-front cell shrinkage (approx. 1 mm/120 s) and a 'high' ice-front velocity for induction of intracellular ice (1 mm/60 s). Usually, with a gap between the Peltiers of 5–6 mm, the ice-front velocity could be fairly well controlled by decreasing the temperature of only one of the Peltier elements. The temperature difference between the two Peltier elements was 20–30 °C.

Image processing. During a freeze-thaw cycle the cell strands were observed through a microscope with 25–100× magnification. The microscopic images of the strand were also fed to a low-light-level camera (Siemens K 5 B, Restlichtkamera) and were continuously videotaped using a commercial tape recorder. Cells were illuminated with epifluorescence optics with interposed brief periods, during which the strands were illuminated with bright-field optics (Nomarski interference contrast) in order to detect cell darkening by IIF. For measuring the degree of shrinkage, selected images of cell strands before and after freeze-induced cell shrinkage were digitized (Frame Grabber, Vision Plus) and either stored on the computer or displayed on the screen of a video monitor. Outlines of all individual cells of a strand were drawn directly on the screen. From the superimposed cross-sections of corresponding shrunken and nonshrunken cells, the size of the shrunken area was measured. If the cell strand changed its position during shrinkage or during re-swelling, the records were rejected. Pixel subtraction was used to facilitate the detection of cell shrinkage along the strand, as described below.

Pixel subtraction. A digitized image of a cell strand with fluorescent cells before freezing, the so-called reference image, was displayed on the screen of a video monitor (fig. 3a). A second digitized image was loaded of the same strand after freeze-induced shrinkage (fig. 3b). An image-processing system (JAVA, Jandel) was used to subtract the gray value of each pixel in the image being loaded from the gray value of each corresponding pixel currently displayed on the video screen. Because in most regions the gray values of the fluorescent cells of both images were almost the same, these areas were displayed as pure black regions in the subtraction image (fig. 3c). However, the nonoverlapping regions, representing the reduction of the cross-sectional areas by freeze-induced shrinkage, were displayed as bright, bandlike areas. Here only the low gray values of the background had been subtracted. This 'subtraction image' was stored on the computer, and the reference image was again displayed on the screen. By subtracting the pixels of the subtraction image from the reference image 2 to 3 times, the shrunken regions in all cells became inserted into the reference image of the strand as black peripheral bands with high contrast (fig. 3d). When images consisted of predominantly dark regions, as in fig. 4b, the pixels of the subtraction image were added instead of subtracted, displaying the shrunken regions now as white bands for better contrast.

Results

After equilibrating salivary gland cells for 15–20 min with fluorescein-containing saline, most cells exhibited bright green fluorescence when excited with blue light

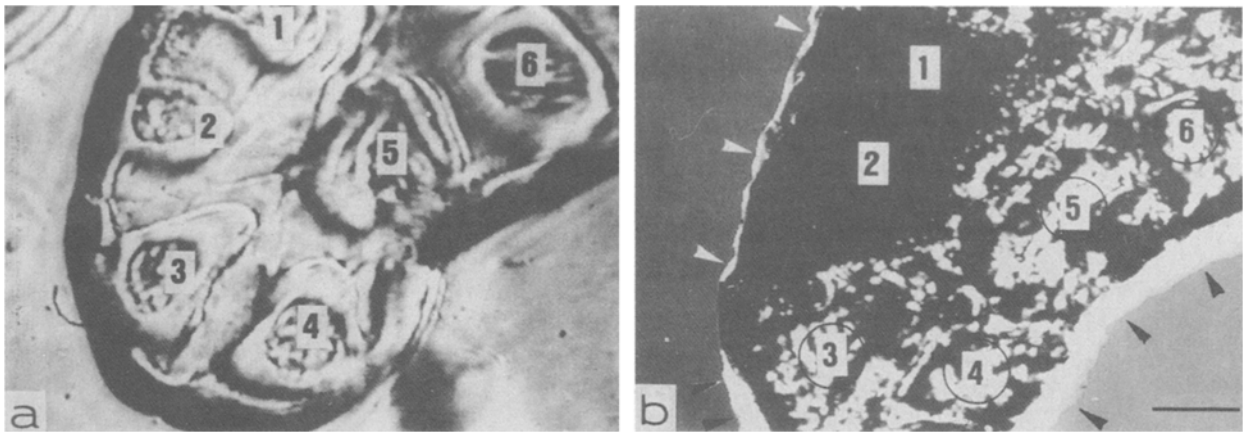

Figure 4. (*a*) A segment of a salivary gland with six cells numbered 1 to 6 before freezing. (*b*) The same segment after encapsulation by ice. Intracellular ice has formed in cells 1 and 2. The degree of pre-ice-front shrinkage is indicated in this micrograph by the white line surrounding the cell strand (marked by arrowheads). The internally frozen cells 1 and 2 had shrunken much less before the advancing ice front (as indicated by the narrow white band) than had cells 3–6, which did not freeze internally. Bar: 40 µm.

through epifluorescence optics. Fluorescent cells lost the accumulated fluorescein in less than a minute when damaged by a needle. Damaged salivary gland cells also became opaque [5]. The loss of transparency of the cells was always combined with the loss of fluorescence. However, the leakage of fluorescein occurred several minutes before cells became opaque. Nonfluorescent cells were therefore considered to be damaged either during dissection or by freezing. No leakage of fluorescein from adjacent cells into a damaged cell was observed at room temperature. This indicated rapid closure of the intercellular connections between the damaged cell and nondamaged neighbours, similar to the 'healing-over process' observed in cardiac muscle [6].

Cell fluorescence remained visible when cells were covered with extracellular ice. In some experiments the microscopic image became distorted by ice needles. After thawing, all cells became transiently permeabilized, and some fluorescein leaked into the extracellular fluid. The intensity of the remaining cell fluorescence after returning to room temperature was, however, still high. In contrast, cells which were presumably freeze-injured as indicated by their coarse protoplasm, a distorted nucleus and their opacity, lost fluorescence within a fraction of a minute. The maintenance of a high-intensity level of cell fluorescence after a freeze-thaw cycle was taken as a criterion for identifying cells with nondamaged cell membranes. Fading of cell fluorescence and the slow loss of fluorescein probably by exocytosis during a freeze-thaw cycle required a relatively high initial concentration of fluorescein in the cells. Cell strands were therefore exposed for at least 15–20 min to the fluorescein-containing saline. After this time all cells appeared uniformly fluorescent (fig. 2b). In bright-field illumination (fig. 2a) a columnar region of the cell can be identified which connects upper and lower flat lobes [7]. No such structural details were visible in through-focus series with the microscope in fluorescent cells treated as described above. In cells which were incubated for shorter periods than 15 min, the central cell regions became visible with an Ω-shaped contour (fig. 2c).

Freeze-induced cell shrinkage. When the cells were optically sectioned using interference contrast optics, the degree of freeze-induced shrinkage of salivary cells was different in different focal planes. In the flat lobes at the top and bottom regions of the cell [7] the degree of shrinkage was larger than in the central portions. The freeze-induced shrinkage of fluorescent cells occurred preferentially at the two faces which were in contact with the ice or the salt profiles ahead of the ice front (fig. 3c and d). The length of the strands did not shorten very much. The observed shrinkage of fluorescent cells appeared to be related to the shrinkage of the upper lobes of the cells and was proportional but larger than the total shrinkage of the cell. The exact relationship of this apparent shrinkage to the total osmotic water loss of the cells is not known. With the pixel-by-pixel subtraction technique, the spatial pattern of shrinkage along the strand was made visible as black marginal bands in the cell strands (fig. 3a–d).

Pre-ice-front shrinkage and IIF. When the temperature was lowered and an advancing ice front had developed in the experimental chamber, in many cases cell shrinkage started long before the ice touched the first cell. This phase was called pre-ice-front shrinkage. Shrinkage continued when the cells were encapsulated by extracellular ice. Pre-ice-front shrinkage was probably caused by the accumulation of solutes which build up ahead of an advancing planar ice front [8]. When the cell strand was in a horizontal position, as in figure 3, the last cell of this strand (consisting of seven cells) began to shrink when the planar ice front was still 100 µm away from the first cell. We estimate that the pre-ice-front shrinkage contributed a substantial fraction to total freeze-induced cell shrinkage.

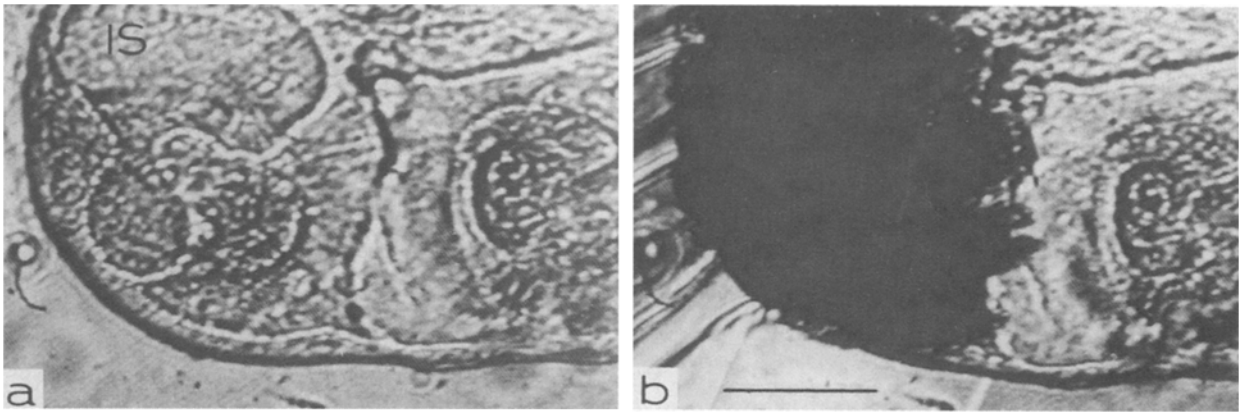

Figure 5. (*a*) Micrograph of three cells of a strand in bright-field illumination (Nomarski interference contrast). Cell boundaries and intercellular spaces (IS) are visible. (*b*) The same cells now covered with extracellular ice. Two cells are black, while the adjacent cell which had not formed intracellular ice has become darker by shrinkage and encapsulation by ice but is still much more transparent than the internally frozen cells. Bar: 40 µm.

Cells with a small degree of pre-ice-front shrinkage also preferentially formed intracellular ice (fig. 4). A two-step image-processing procedure was used to demonstrate both the degree of pre-ice-front shrinkage and the occurrence of intracellular ice (fig. 4b): by moving an ice front close to the first cell of the gland segment, the degree of pre-ice-front shrinkage could be assessed. The resulting subtraction image was stored on the computer. To induce IIF, the ice front was moved again towards, and this time across, the gland segment. Intracellular ice was detected in two cells. Because the bright-field image of the gland segment under ice was relatively dark, the pixels from the area of pre-ice-front shrinkage were added instead of subtracted (as with fluorescent cells). Repeating the 'adding procedure' three times made it possible to see both pre-ice-front shrinkage (marked by arrowheads in fig. 4b) and intracellular ice distribution on the same image.

Internal ice formation in salivary gland cells was indicated by a sudden darkening, as reported for other cells [9]. Darkening of internally frozen cells was more intense than the darkening caused by dehydration or after the cells were covered with ice crystals (fig. 5). In cell strands in which the saliva had not been washed out from interstitial spaces, cells and frozen saliva had almost the same degree of darkening, which made it difficult to identify internal cell freezing.

Cell-to-cell propagation of intracellular ice. When the long axis of the cell strand was perpendicular to the advancing ice front, cells were exposed sequentially to increasing solute concentration and encapsulation by ice.

To expose all cells simultaneously to the same temperatures and salt profiles, the strands were placed in a vertical position, with the strand axis parallel to the approaching ice front (as in figs 2c, 6 and 7). The temperature gradient applied was 3.6–3.7 °C/mm, and the nucleation temperature was −12 to −14 °C. After ice had formed in one cell, it was frequently observed that adjacent cells also became black in rapid sequence. Darkening often spread from one cell in both directions of the strand. Propagation of ice was interrupted by short delays. The average time delay between subsequent cell darkening was in the range of 200–300 ms. The sequence of micrographs of figure 6 shows the cell-to-cell spread of intracellular ice. After extracellular ice had encapsulated all cells, internal freezing developed in a cell at the lower end of the strand (fig. 6a). Within a fraction of a second intracellular ice propagated perpendicular to the thermal gradient to five neighbouring cells (fig. 6b–f). Ten out of 14 strands studied in this experimental arrangement showed successive darkenings between adjacent cells with regular time delays.

Damaged (nonfluorescent) cells also darkened when extracellular ice was present. However, in contrast to the spontaneous IIF in undamaged cells which developed after all cells were encapsulated by ice, damaged cells darkened immediately after extracellular ice had touched them. Presumably, the extracellular ice invaded such cells through defects in the cell membranes. To eliminate this type of cell darkening from our data, the integrity of the cell membranes at temperatures at which IIF could be expected was frequently checked up. Only darkening of cells with a persistent and bright fluorescence and which occurred after encapsulation by ice were considered to be caused by spontaneous IIF.

IIF and intercellular coupling. Salivary gland cells are extensively coupled by gap-junctional (nexus) channels and have been frequently selected for studies of intercellular communication [10, 11]. Channels between cells can be blocked by exposing the cells to dinitrophenol (DNP) [3] or to heptanol [12, 13]. In 6 strands in which cells were pretreated by $2–8 \times 10^{-4}$ mol/l of DNP for 40 to 60 min or in 11 strands pretreated by 3×10^{-3} mol/l of heptanol (cell strand parallel to the approach-

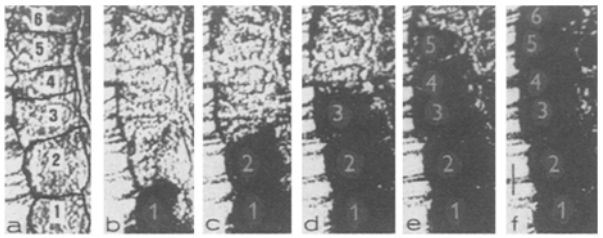

Figure 6. Cell-to-cell propagation of intracellular ice. (*a*) The cell strand was covered by extracellular ice (cell boundaries have been redrawn). (*b*) Darkening in a cell numbered 1 indicates intracellular ice formation. (*c*) After 200 ms intracellular ice had propagated to the adjacent cell 2. (*d–f*) Intracellular ice had spread from cell to cell and has finally reached cell 6 at the top of the strand. Ice propagation from cell 1 to cell 6 took less than a second. Time delays between sequential darkening were between 150 and 220 ms. Bar: 40 µm.

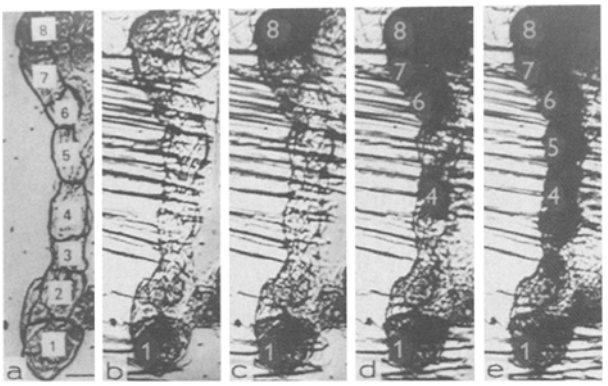

Figure 7. Micrographs showing patterns of cell darkening in decoupled cells. Cells of this strand had been decoupled by DNP. The temporal and spatial patterns of cell darkening were now random. After internal freezing had occurred in a cell numbered 1 (*b*), the next cell, numbered 8, at the opposite end of the strand froze internally (*c*). After a time delay of more than a second, cells 6, 4 and 7 formed intracellular ice (*d*). After a further delay cell 5 darkened (*e*). Cells 2 and 3 did not form intracellular ice. Bar: 40 µm.

ing ice front), the spatial pattern of cell darkening was random, and/or the time intervals between consecutive cell darkenings were irregular. Figure 7 illustrates the random spread of ice along the cell strand exposed to DNP. Darkening began in the cell numbered 1 at the lower end of the strand (fig. 7b), then occurred in a cell numbered 8 at the opposite end of the strand (fig. 7c). After a time delay of more than a second, cells 6, 4 and 7 became dark (fig. 7d), and finally cell 5 formed intracellular ice (fig. 7e). While the propagation of ice in coupled cells was interrupted by time delays of constant duration, decoupled cells sometimes froze simultaneously, or variable time delays lasting between less than 50 ms and 3 s were interposed between successive darkenings.

The formation of intracellular ice was dependent on the velocity of the approaching ice front (i.e. on the cooling rate). At velocities between 1 mm/120 s and 1 mm/90 s either no intracellular ice was formed or only one or two cells froze internally without ice propagation. However, at velocities about 1 mm/60 s the cell-to-cell propagation of ice was a frequent event.

Discussion

In a network of cells arranged in three dimensions as in normal tissues, individual cells usually cannot be identified. The cell chains which have been used in this study lack the mechanical attachments and connecting junctions to other cells in the second and third dimensions. Freeze-induced shrinkage of cells in normal tissues may be different from that in a one-dimensional strand; however, the cell strand does offer the chance to observe individual cells attached to each other during freezing and to obtain experimental results that may have relevance for freeze-induced cell shrinkage inside tissue. The influence of intercellular channels on IIF as well as the spatial extension of freeze-induced shrinkage can be expected to be qualitatively similar in tissues and strands. For these questions we have considered the cell strand to represent a simple model of tissue.

Salivary glands contain large peripheral cells which have frequently been used for studies of intercellular coupling [10, 11]. However, the whole gland was unsuitable for our experiments. During exposure to hypertonic media or during freezing, the gland shrinks in toto, and the resulting cell movements impeded the analysis of the shrinkage of individual cells. Furthermore, the saliva inside the gland also became fluorescent after exposure to fluorescein-containing solutions, which obscured cell outlines. We therefore dissected cell strands out of the gland, washing out the saliva prior to freezing. A further advantage of using a strand is that these cells, in contrast to those in the gland, are exposed simultaneously at their apical and basal faces to the salt profiles ahead of an advancing ice front. During the dissection procedures or during the transfer to the freezing chamber, cells may be damaged. Extracellular ice penetrates damaged cells, which then become black in bright-field illumination and cannot be distinguished from cells which spontaneously form intracellular ice at nucleation temperature. Therefore, an indicator for the integrity of cell membranes before internal ice formation had to be found. Damaged cells become opaque, which can be best seen under a stereomicroscope at low magnification. At higher magnification the loss of transparency can hardly be detected. We observed accidentally that noninjured salivary gland cells accumulate fluorescein when exposed to saline containing sodium fluorescein, while injured cells do not. Fluorescent cells lose accumulated fluorescein rapidly when damaged. Leakage of fluorescein was found to occur before the loss of transparency could be detected. Therefore, the persistence of a bright cell fluorescence, for instance

after freezing, was used as an indicator for identifying cells with intact membranes. The mechanism by which fluorescein entered the cells is not known. Preliminary electron microscopic studies support the assumption that extracellular fluorescein is transported into cells via pinocytosis. We observed that for the identification of intact salivary gland cells, fluorescein diacetate (FDA) is not a good choice. Cells which were obviously damaged, as judged by their loss of transparency, often exhibited bright fluorescence after exposure to FDA-containing saline.

Pre-ice-front shrinkage was presumably caused by solute redistribution ahead of an advancing ice front. The spatial distribution of such salt profiles has been extensively analysed [8]. Though we cannot correctly calculate how much of the total freeze-induced shrinkage is contributed by pre-ice-front shrinkage, it appears to be a substantial fraction. Cells of strands positioned as in figure 2c (strand axis parallel to the ice front) will be simultaneously exposed to decreasing temperatures and to the increasing solute concentration ahead of the planar ice front. Cells with a small degree of pre-ice-front shrinkage often did not dehydrate as much after encapsulation with ice as cells which had developed regular pre-ice-front shrinkage. At nucleation temperature the probability of IIF should therefore be increased in cells with little pre-ice-front shrinkage. This was indeed observed to occur in the gland segment shown in figure 4b. The results suggest that pre-ice-front shrinkage has a significant influence on IIF and on the degree of cryopreservation of tissues.

According to the recent physicochemical model of IIF [14], in the presence of external ice the plasma membrane may be an energetically favourable site for heterogeneous nucleation. This so-called surface-catalysed nucleation (as opposed to volume-catalysed nucleation) is active between -5 and -20 °C. The temperature range of -12 to -14 °C for intracellular ice nucleation observed in our experiments falls within the range mentioned above.

The main finding concerning IIF in our study is the demonstration of two types of intercellular ice propagation along the strand of cells exposed simultaneously to the ice front: (1) the propagation of ice from one cell to the next adjacent cell with regular time intervals between consecutive cell darkenings. This type was characteristic for cell strands prepared carefully and kept in a normal saline—the conditions under which a high degree of electrical coupling between cells was observed [3, 10, 11] (unpubl. obs.); (2) the random spread of ice jumping from one end of the strand to the opposite end and/or with irregular time intervals between consecutive cell darkenings even in case of ice spread between adjacent cells. This type was characteristic for cell strands exposed to DNP or heptanol—known uncoupling agents [3, 12, 13].

Ice propagation between adjacent cells has also been observed in fibroblasts, and it has been reported that cell-to-cell contact facilitates intracellular nucleation between adjacent fibroblasts [15]. One may argue that the apparent cell-to-cell propagation of ice between adjacent cells in strands prepared under normal conditions was in fact no propagation but may have been caused by a time-shifted spontaneous development of internal freezing in adjacent cells. However, it appears unlikely that this event occurs in a strand of 6 to 10 adjacent cells with short and regular time delays. We therefore consider a cell-to-cell propagation of intracellular ice via nexus (gap-junctional) channels to be a more likely explanation. The whole experimental setup in our study did not allow current monitoring of cell coupling with electrical measurements or with diffusion of dyes.

The possibility of the penetration of ice crystals through pores in the cell membrane has been analysed and discussed by P. Mazur [16, 17]. According to his calculations, ice crystals from extracellular ice will not grow through ion channels which have radii of 0.3–0.4 nm. His calculations were, however, based on several assumptions. Changing the assumed value of the contact angle between ice and the pore wall from 0° to 75° would permit ice crystals to grow through channels with a radius of 0.7 nm. Intercellular nexus channels have radii of 0.8–1.0 nm in mammalian cells and 1.0–1.5 nm in insect cells [18–20] and may therefore allow the growth of ice crystals from one cell to adjacent cells. Differences between nexus channels are due not only to interspecies differences but to differential expression of connexins [21]. The different pattern of connexin distribution and its importance for the control of secretory cell function have been described in a comparative study of 10 exocrine and endocrine glands [22].

The mechanism of IIF as discussed recently [14, 23] is relevant to the formation of ice in one cell. When this has happened, we assume that the ice crystals can penetrate the gap-junctional channels in the manner suggested by Mazur [16, 17].

If the spread of intracellular ice also occurs in other tissues during freezing, it would contribute to the freeze injury of the tissues. The number of lethally freeze-damaged cells would be increased by the propagation of intracellular ice. One would expect a higher survival rate for cells which were frozen when isolated from each other than for cells which are connected by channels as in most tissues. For cardiac muscle, in which the cells are coupled by numerous junctions, this phenomenon has indeed been observed. Survival rates of isolated cardiac muscle cells frozen in suspension were high [24]. However, when cardiac muscle cells were frozen in small muscular bundles, all cells suffered from severe freezing damage and could no longer be activated [25, 26].

In conclusion, we believe that the results obtained in this study are relevant for both cryoconservation of cells

in tissue and cryodestruction of malignant tumour cells, which in most cases are distinguished by depressed intercellular coupling [2].

Acknowledgements. The authors would like to thank Dr T. Plant for reviewing the manuscript. A preliminary account of this work was presented at the 29th meeting of the Society for Cryobiology, Ithaca, New York, 14–19 June 1992. This work was supported, in part, by the Slovak grant agency for science (grants no. 2/1313/95 and 95/5305/515).

1 Mazur P. (1963) Kinetics of water loss from cells at subzero temperatures and the likelihood of intracellular freezing. J. Gen. Physiol. **47:** 347–369
2 Loewenstein W. R. (1986) Cell-to-cell communication. Permeability, regulation, formation, and functions of the cell-cell membrane channel in cell junctions. In: Physiology of Membrane Disorders, pp. 329–343, Andreoli T. E., Hoffman J. F., Fanestil D. D. and Schultz S. G. (eds), Plenum Publishing Corporation, New York
3 Politoff A. L., Socolar S. J. and Loewenstein W. R. (1969) Permeability of a cell membrane junction. Dependence on energy metabolism. J. Gen. Physiol. **53:** 498–515
4 Rubinsky B., Arav A. and Devries A. L. (1991) Cryopreservation of oocytes using directional cooling and antifreeze glycoproteins. Cryo-Letters **12:** 93–106
5 Loewenstein W. R. and Kanno Y. J. (1964) Studies on an epithelial (gland) cell junction. I. Modifications of surface membrane permeability. J. Cell Biol. **22:** 565–586
6 Engelmann T. W. (1877) Vergleichende Untersuchungen zur Lehre von der Muskel- und Nervenelektricität. Arch. Ges. Physiol. **15:** 116–148
7 Kloetzel J. A. and Laufer H. J. (1969) A fine-structural analysis of larval salivary gland function in *Chironomus thummi* (Diptera). J. Ultrastruct. Res. **29:** 15–36
8 Körber C., Scheiwe M. W. and Wollhöver K. (1983) Solute polarization during planar freezing of aqueous salt solutions. Int. J. Heat Mass Transfer **26:** 1241–1253
9 Leibo S. P., McGrath J. J. and Cravalho E. G. (1978) Microscopic observation of intracellular ice formation in mouse ova as a function of cooling rate. Cryobiology **15:** 257–271
10 Loewenstein W. R., Socolar S. J., Higashino S., Kanno Y. and Davidson N. (1965) Intercellular communication: renal, urinary bladder, sensory, and salivary gland cells. Science **149:** 295–298
11 Loewenstein W. R., Nakas M. and Socolar S. J. (1967) Junctional membrane uncoupling. Permeability transformations at a cell membrane junction. J. Gen. Physiol. **50:** 1865–1891
12 Johnston M. F., Simon F. A. and Ramón F. (1980) Interaction of anaesthetics with electrical synapses. Nature **286:** 498–500
13 Bernardini G., Peracchia C. and Peracchia L. L. (1984) Reversible effects of heptanol on gap junction structure and cell-to-cell electrical coupling. Eur. J. Cell Biol. **34:** 307–312
14 Toner M., Cravalho E. G. and Karel M. (1990) Thermodynamics and kinetics of intracellular ice formation during freezing of biological cells. J. Appl. Phys. **67:** 1582–1593
15 Larese A., Yang H., Petrenko A. and McGann L. E. (1992) Intracellular ice formation is affected by cell-to-cell contact. Cryobiology **29:** 728, abstract 69
16 Mazur P. (1965) The role of cell membranes in the freezing of yeast and other single cells. Ann. N. Y. Acad. Sci. **125:** 658–676
17 Mazur P. (1966) Physical and chemical basis of injury in single-celled microorganisms subjected to freezing and thawing. In: Cryobiology, pp. 213–315, Meryman H. T. (ed.), Academic Press, London
18 Simpson I., Rose B. and Loewenstein W. R. (1977) Size limits of molecules permeating the junctional membrane channels. Science **195:** 294–296
19 Flagg-Newton J. L., Simpson I. and Loewenstein W. R. (1979) Permeability of the cell-to-cell membrane channels in mammalian cell junction. Science **205:** 404–407
20 Schwartzmann G. O. H., Wiegandt H., Rose B., Zimmerman A., Ben-Haim D. and Loewenstein W. R. (1981) The diameter of the cell-to-cell junctional membrane channels, as probed with neutral molecules. Science **213:** 551–553
21 Meda P. (1994) Molecular biology of gap junction proteins. In: Molecular Biology of Diabetes, part 1, pp. 333–356, Draznin B. and LeRoith D. (eds), Humana Press, Totowa, NJ
22 Meda P., Pepper M. S., Traub O., Willecke K., Gros D., Beyer E., Nicholson B., Paul D. and Orci L. (1993) Differential expression of gap junction connexins in endocrine and exocrine glands. Endocrinology **133:** 2371–2378
23 Bryant G. (1995) DSC measurement of cell suspensions during successive freezing runs: implications for the mechanisms of intracellular ice formation. Cryobiology **32:** 114–128
24 Bustamante J. O. and Jachimowicz D. (1988) Cryopreservation of human heart cells. Cryobiology **25:** 394–408
25 Berger W. K. (1987) Effects of sub-zero temperatures on conduction of action potentials in atrial bundles of the frog heart. Cryo-Letters **8:** 7–20
26 Berger W. K. and Tovar O. (1990) On the mechanism of the freeze-induced conduction block of action potentials in rat cardiac muscle. Cryo-Letters **11:** 35–48